



Silver(I), palladium(II) and mercury(II) NHC complexes based on bis-benzimidazole salts with mesitylene linker: Synthesis, structural studies and catalytic activity

Qing-Xiang Liu^{a,b,*}, Li-Xuan Zhao^{a,b}, Xiao-Jun Zhao^{a,b}, Zhi-Xiang Zhao^{a,b}, Zhi-Qiang Wang^{a,b}, Ai-Hui Chen^{a,b}, Xiu-Guang Wang^{a,b}

^aTianjin Key Laboratory of Structure and Performance for Functional Molecules, Key Laboratory of Inorganic–Organic Hybrid Functional Material Chemistry, Ministry of Education, College of Chemistry, Tianjin Normal University, Tianjin 300387, China

^bState Key Laboratory of Elemento-organic Chemistry, Nankai University, China

ARTICLE INFO

Article history:

Received 22 November 2012

Received in revised form

24 January 2013

Accepted 30 January 2013

Keywords:

Carbene

Silver

Mercury

Palladium

Catalysis

ABSTRACT

The diimidazolium salts bis[1-R-imidazoliumylmethyl]mesitylene-2X (**1**: R = PhCH₂, X = Br[−] and **2**: R = Et, X = PF₆[−]) and the dibenzimidazolium salts bis[1-R-benzimidazoliumylmethyl]mesitylene-2X (**3**: R = Et, X = PF₆[−]; **4**: R = PhCH₂, X = I[−]), as well as their four NHC silver(I), palladium(II) and mercury(II) complexes, {[mesitylene(CH₂imyPhCH₂)₂Ag₂·Ag₂Br₄]_n (**6**), {mesitylene[(CH₂imyPhCH₂)PdCl₂(CH₃CN)]₂} (**7**), {mesitylene[(CH₂imyEt)₂Hg₂(CHCN)][HgI₄]} (**8**) and {[mesitylene(CH₂bimyⁿPr)₂HgI][HgI₄]_{0.5}} (**9**), as well as one anionic complex {[1,3-bis(1-benzylbenzimidazole)methyl]mesitylene][HgI₄]} (**5**) (imy = imidazol-2-ylidene and bimy = benzimidazol-2-ylidene), have been prepared and characterized. In the complex **6**, the macrometallo-cycles formed by two precursor **1** and two silver(I) atoms are connected together via Ag₂Br₄ unit to form a 1D polymeric chain. Complex **7** adopted an open structure formed by one precursor **1** and two Pd(II) atoms. In complex **8**, a bidentate dicarbene from precursor **2** and a doubly deprotonated acetonitrile coordinate with two Hg(II) atoms to afford a funnel-like structure. The 10-membered macrometallo-cycle of **9** was formed by one precursor **3** and one Hg(II) atom. In the crystal packings of these compounds, 1D supramolecular chains, 2D supramolecular layers or 3D architectures are formed via intermolecular weak interactions, including π–π interactions, hydrogen bonds, C–H···π contacts and weak Hg···N and Hg···I bonds. Additionally, the catalytic activity of the NHC palladium(II) complex **7** in Suzuki–Miyaura cross-coupling reaction was studied.

© 2013 Elsevier B.V. All rights reserved.

1. Introduction

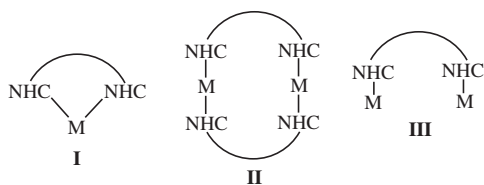
The transition metal complexes of N-Heterocyclic carbenes (NHCs) have attracted considerable interest over the past two decades due to their structural variety and easy access through deprotonation of N, N′-disubstituted imidazolium (or benzimidazolium) salts [1–4]. The strong σ-donating ability of N-heterocyclic carbenes leads to high stability of their metal complexes toward heat, moisture and air. More recently, much effort has also been devoted to the synthesis of functionalized NHC ligands and their metal complexes [5–9]. In the family of N-heterocyclic carbenes,

many bidentate bis-NHC ligands have been reported, in which a pair of NHC moieties are connected by a bridging linker, such as phenylene [10–16], pyridyl and lutidinyl [17–19], ether chain [20–23] and alkyl [24–29]. These NHC ligands with different bridging linkers can form mainly three types of metal complexes (Scheme 1), namely, the monometal monoligand macrocycle (I), the dimetal diligand macrocycle (II) and the open structure composed of one bidentate dicarbene ligand and two metal atoms (III). These different conformations of complexes are related to the flexibility and size of bridging linkers. Additionally, the steric hindrance of N-substitutes on imidazole rings, and the difference of benzimidazole ring and imidazole ring have also some influence on the structures of complexes.

Among NHC-metal complexes, the NHC silver(I) [30–32], mercury(II) [33–35] and palladium(II) [36–39] complexes have played important roles in the development of the N-heterocyclic carbene chemistry. N-heterocyclic carbene silver(I) complexes can be used as

* Corresponding author. Tianjin Key Laboratory of Structure and Performance for Functional Molecules, Key Laboratory of Inorganic–Organic Hybrid Functional Material Chemistry, Ministry of Education, College of Chemistry, Tianjin Normal University, Tianjin 300387, China.

E-mail addresses: tjnulqx@163.com, qxliu@you.com (Q.-X. Liu).



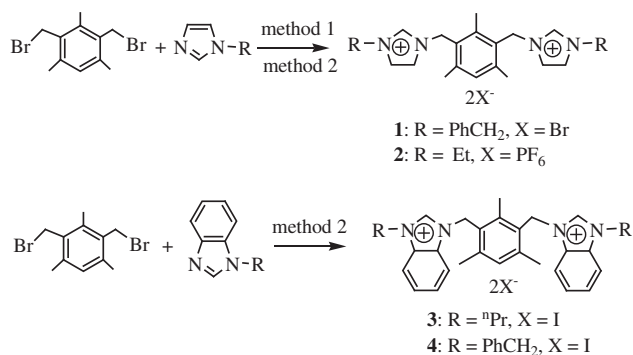
Scheme 1. The conformations of NHC metal complexes.

carbene transfer reagents to make other NHC metal complexes, such as Ni, Pd, Pt, Cu, Au, Rh, Ir and Ru carbene complexes [40–43]. Some N-Heterocyclic carbene mercury(II) complexes possess interesting structures [44,45]. Particularly, N-Heterocyclic carbene palladium(II) complexes have been demonstrated to be efficient catalysts for some organic reactions, such as Suzuki–Miyaura and Heck cross-coupling reactions [46–50]. In order to understand further the influence of bridging linkers, N-substitutes, imidazole ring and benzimidazole ring on the conformations and the crystal packings of complexes, we inhere reported the synthesis, structures and fluorescent emission spectra of four new NHC-metal complexes, {[mesitylene(CH₂imyPhCH₂)₂Ag₂·Ag₂Br₄]_n (**6**), {mesitylene[(CH₂imyPhCH₂)PdCl₂(CH₃CN)]₂ (**7**), {mesitylene[(CH₂imyEt)₂Hg₂(CHCN)][HgI₄]} (**8**) and {mesitylene[(CH₂bimyⁿPr)₂HgI][HgI₄]_{0.5}} (**9**), as well as one anionic complex {[1,3-bis(1-benzylbenzimidazoliumethyl)mesitylene][HgI₄]} (**5**) (imy = imidazol-2-ylidene and bimy = benzimidazol-2-ylidene). Additionally, we also describe the diverse conformations of precursors **1–4** and their complexes **5–9**. Moreover, the catalytic performance of NHC palladium(II) complex **7** in Suzuki–Miyaura cross-coupling reaction was studied.

2. Results and discussion

2.1. Synthesis and general characterization of diimidazolium (or dibenzimidazolium) salts **1–4**

The diimidazolium salt, bis[1-benzyl-imidazoliumylmethyl]mesitylene bromide (**1**) was prepared from imidazole by alkylation with benzyl bromide followed by quarterization with 1,3-bis(bromomethyl)mesitylene in sequence (method 1 of Scheme 2). Bis[1-ethyl-imidazoliumylmethyl]mesitylene hexafluorophosphate (**2**) was obtained via two steps of reactions. The first step is in a manner analogous to that of **1**, and the second step is the anion exchange with ammonium hexafluorophosphate in methanol (method 2 of Scheme 2). Bis[1-R-benzimidazoliumylmethyl]mesitylene iodide (**3**: R = ⁿPr, **4**: R = PyCH₂) were prepared in a manner



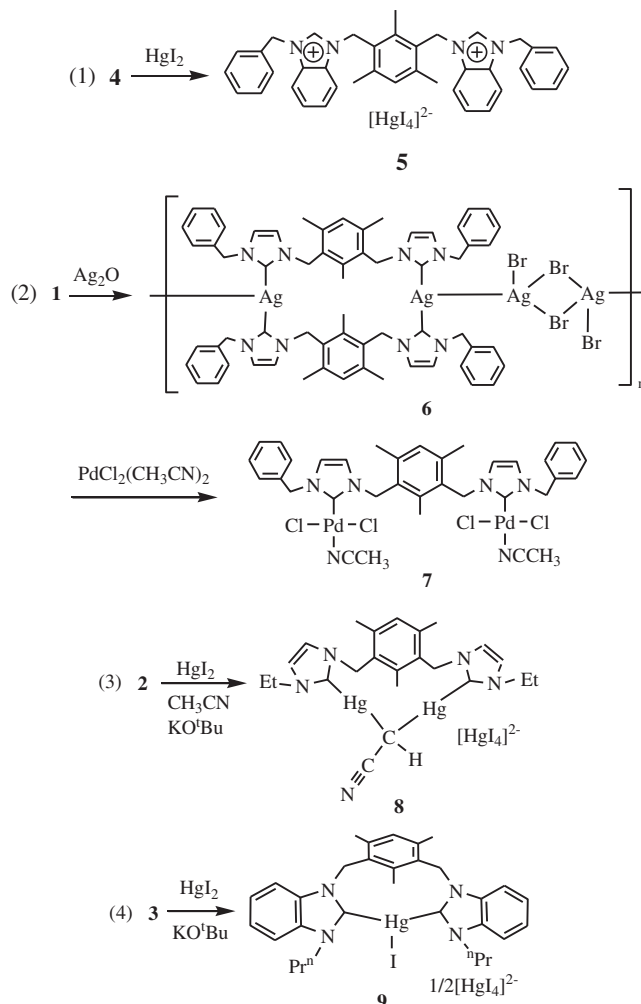
Reagents: method 1 for **1**, THF, reflux.
method 2 for **2–4**, (i) THF, reflux; (ii) anionic exchange with NH₄PF₆ in methanol for **2**, and with NaI in acetone for **3** and **4**.

Scheme 2. Preparation of precursors **1–4**.

analogous to that of **2**, only instead of ammonium hexafluorophosphate with sodium iodide in the second step (method 2 of Scheme 2). Precursors **1–4** are stable toward air and moisture, soluble in polar organic solvents such as dichloromethane, acetonitrile and methanol, and almost insoluble in benzene, diethyl ether and petroleum ether. In the ¹H NMR spectra of **1–4**, the imidazolium (or benzimidazolium) proton signals (NCHN) appear at δ = 8.32–9.77 ppm, which is consistent with the chemical shifts of reported imidazolium (or benzimidazolium) salts [5–9].

2.2. Synthesis and general characterization of complexes **5–9**

Synthetic methods of complexes **5–9** are shown in Scheme 2. The precursor **4** was treated with anhydrous mercury(II) iodide to afford anionic complex [1,3-bis(1-benzylbenzimidazoliumethyl)mesitylene][HgI₄] (**5**) (Scheme 3(1)). The reaction of **1** with silver(I) oxide afforded 1D polymeric chain {[mesitylene(CH₂imyPhCH₂)₂Ag₂·Ag₂Br₄]_n (**6**) bearing 20-membered macro-metallo-cycles and Ag₂Br₄ units. The reaction of complex **6** with [PdCl₂(CH₃CN)]₂ via the transformation of metal gave the complex {mesitylene[(CH₂imyPhCH₂)PdCl₂(CH₃CN)]₂ (**7**) with an open structure (Scheme 3(2)). The precursor **2** was treated with anhydrous mercury(II) iodide in the presence of KO^tBu in CH₃CN to afford complex {mesitylene[(CH₂imyEt)₂Hg₂(CHCN)][HgI₄]} (**8**) (Scheme 3(3)). The precursor **3** was treated with anhydrous



Scheme 3. Preparation of complexes **5–9**.

mercury(II) iodide in the presence of KO^tBu in CH_2Cl_2 to afford complex $\{[\text{mesitylene}(\text{CH}_2\text{bimy}^n\text{Pr})_2\text{HgI}][\text{HgI}_4]_{0.5}\}$ (**9**) (Scheme 3(4)). The complexes **5–9** are stable toward air and moisture, soluble in DMSO and insoluble in diethyl ether and hydrocarbon solvents. The NHC silver(I) complex **6** is slightly light sensitive. In the ^1H NMR spectra of **6–9**, the disappearance of the resonances for the imidazolium (or benzimidazolium) protons (NCHN) shows the formation of the expected metal carbene complexes, and the chemical shifts of other protons are similar to those of the corresponding precursors. The ^1H NMR spectrum of anionic complex **5** is similar to that of the corresponding precursor **4**. For ^{13}C NMR spectra, the signals of the carbene carbon in complexes **6–9** appear at 153.3–184.1 ppm, which are similar to the reported carbene metal complexes [30–39].

2.3. Structures of diimidazolium salt **2** and complexes **5–9**

Molecular structure of the precursor **2** and complexes **5–9** were demonstrated by X-ray analysis. The crystals of **2**, **5**, **6**· $4\text{CH}_3\text{CN}$, **7**· H_2O , **8** and **9** suitable for X-ray diffraction were obtained by slow diffusion of diethyl ether into their DMSO/ CH_3CN solutions.

In precursor **2** and complex **6**, two [Rimy] arms on the same ligand lie in the opposite sides of the mesitylene plane due to steric hindrance (Fig. 1(a) and Fig. 3(b)). In contrast, two [Rimy] (or [Rbimy]) arms on the same ligand of complexes **5** and **7–9** are placed in the same side of the mesitylene plane (Fig. 2(a) and Fig. 4(a)–6(a)). In precursor **2** and complexes **5–9**, two imidazole (or benzimidazole) rings on the same ligand form the dihedral angles of 14.3–86.7° (Table 1). The mesitylene plane and two imidazole (or benzimidazole) rings on the same ligand form the dihedral angles of 75.6–89.1°. The dihedral angles between imidazole (or benzimidazole) ring and adjacent benzene ring of benzyl group (or pyridine ring) in **5–7** are 68.8–88.4°. In complexes **6–9**, the internal ring angles (N–C–N) at the carbene centers are in the range of 104.5–108.4°, which are comparable to those of the known NHC–metal complexes [30–39], but these values are slightly smaller than those of precursor **2** (109.5°) and anionic complex **5** (110.5°).

In precursor **2**, one cationic entity and two hexafluorophosphate anions are held together via two C–H···F hydrogen bonds (Fig. 1(a)). In hydrogen bonds, the hydrogen atoms are from

imidazole rings (the data of hydrogen bonds being given in Table 2). These data of hydrogen bonds are comparable with those reported [51]. The heads of two imidazole rings point to opposite directions.

In anionic complex **5**, a 12-membered macrocycle is formed by one dibenzimidazole cation unit and one iodine atom from $[\text{HgI}_4]^{2-}$ via two C–H···I hydrogen bonds (Fig. 2(a)), in which hydrogen atoms are from imidazole ring (Table 2). In anionic unit $[\text{HgI}_4]^{2-}$, the mercury(II) atom is coordinated to four iodine atoms to form a slightly distorted tetrahedral geometry. The distances of Hg–I bonds vary from 2.641(2) Å to 2.753(3) Å, and the bond angles of I–Hg–I are in the range of 96.7(6)–119.3(5)°.

1D polymeric chain of complex **6** is formed by the cage-like cations and anionic unit Ag_2Br_4 via Ag–Ag bonds (Ag(1)–Ag(2) distance = 2.997(6) Å) as shown in Fig. 3(a). Each cage-like cation is constituted by two bidentate dicarbene ligands and two silver(I) atoms (Fig. 3(b)), in which four benzene rings from four different benzyl groups as the lids of top and bottom to close the cage. In each cage-like structure, two mesitylene planes are nearly parallel with the dihedral angle of 3.4(1)°, and the dihedral angle between the benzene rings of benzyl groups and the benzene rings of mesitylene is in the range of 5.1–18.8°. Two C–Ag–C units are crossed with the torsion angles of C(8)–Ag(4)–Ag(1)–C(39) of 90.3(8)° and C(53)–Ag(4)–Ag(1)–C(22) of 83.8(8)°. Each silver(I) atom in the cage-like cation is tricoordinated with two carbene carbon atoms and another silver(I) atom. The bond angles of two C–Ag–C are 156.5(2)° and 167.0(2)°, respectively, and the distance of Ag–C is in the range of 2.101(5)–2.119(5) Å.

The anionic unit Ag_2Br_4 of **6** is formed by two silver(I) atoms and four bromine atoms (two bridging bromines Br(2) and Br(3), and two non-bridging bromines Br(1) and Br(4)). The coplanar four atoms Ag(2), Br(2), Ag(3) and Br(3) form a quadrangle Ag_2Br_2 arrangement (Br(2)–Ag(2)–Br(3) angle = 97.4(3)° and Ag(2)–Br(2)–Ag(3) angle = 82.7(3)°). The two non-bridging bromine atoms Br(1) and Br(4) lie in both sides of the quadrangle plane (Br(1)–Ag(2)–Br(2) angle = 129.1(3)°). Each silver(I) atom in Ag_2Br_4 unit is tetracoordinated with three bromine atoms and another silver(I) atom. The distance of non-bridging bromine and silver(I) (Ag(2)–Br(1) distance = 2.548(8) Å) is slightly shorter than that of bridging bromine and silver(I) (Ag(2)–Br(2) distance = 2.620(9) Å and Ag(2)–Br(3) distance = 2.802(8) Å). The Ag(2)···Ag(3) separation of 3.543(3) Å in the anionic unit shows no metal–metal

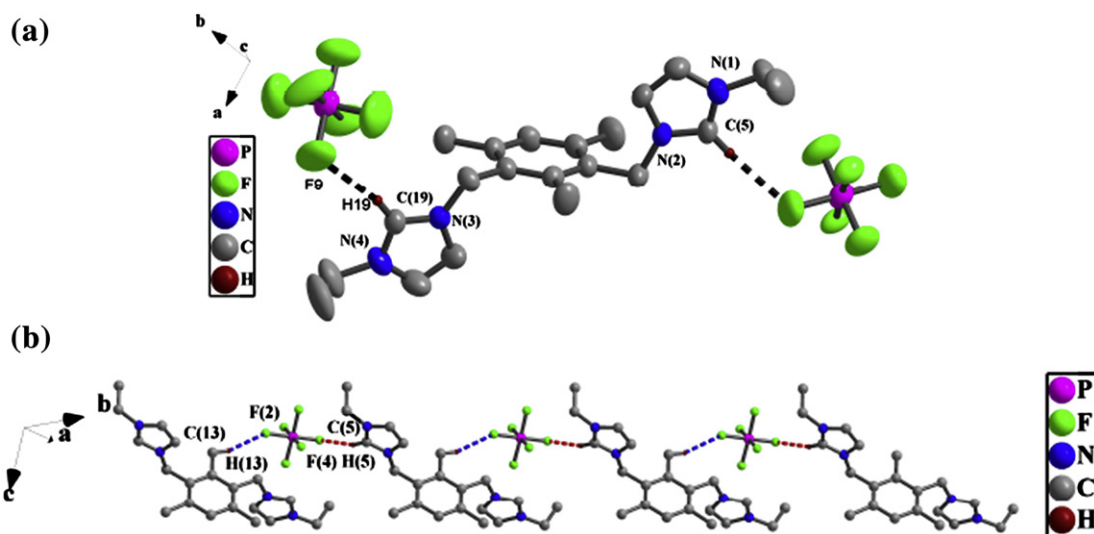


Fig. 1. (a). Perspective view of **2** and anisotropic displacement parameters depicting 50% probability. All hydrogen atoms except those participating in the C–H···F hydrogen bonds were omitted for clarity. Selected bond lengths (Å) and angles (°): N(1)–C(5) 1.311(5), N(2)–C(5) 1.325(4); N(1)–C(5)–N(2) 109.5(3). (b). The 1D supramolecular chain via C–H···F hydrogen bonds. All hydrogen atoms except those participating in the C–H···F hydrogen bonds were omitted for clarity in **2**.

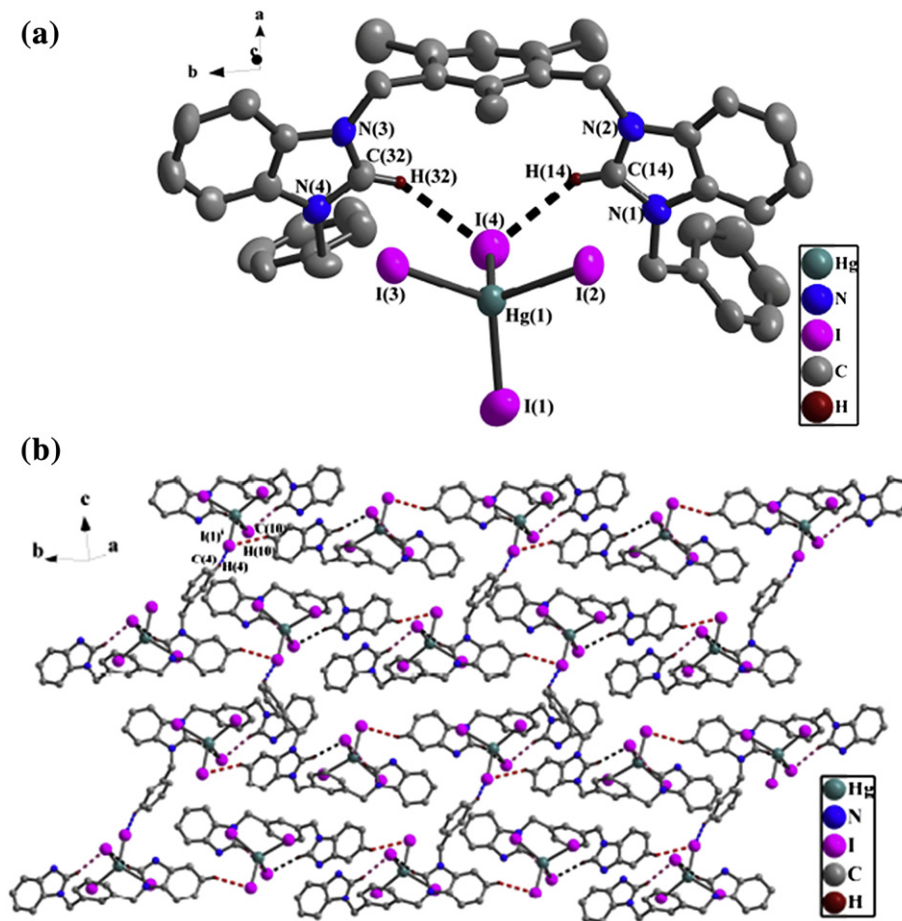


Fig. 2. (a). Perspective view of **5** and anisotropic displacement parameters depicting 50% probability. All hydrogen atoms except those participating in the C–H···I hydrogen bonds were omitted for clarity. Selected bond lengths (Å) and angles ($^{\circ}$): N(1)–C(14) 1.320(1), N(2)–C(14) 1.337(1); N(1)–C(14)–N(2) 110.5(1). (b). The 2D supramolecular layer by C–H···I hydrogen bonds. All hydrogen atoms except those participating in the C–H···I hydrogen bonds were omitted for clarity in **5**.

interactions (the van der Waals radii of silver = 1.7 Å). In 1D polymeric chain, the Ag(1)···Ag(4) separation is 7.420(9) Å.

Similar to precursor **2**, complex **7** is also an open structure, and the difference is that two [benzylimyPdCl₂(NCCH₃)] units in **7** lie in the same side of the mesitylene plane as shown in Fig. 4(a). The X-ray crystal structural analysis of **7** shows that there exist a symmetric plane in the complex. Each palladium atom is tetracoordinated with one carbene carbon atom, one nitrogen atom of acetonitrile and two chlorine atoms to adopt a square *trans* conformation. The N(5)–Pd(1)–C(10) and Cl(1)–Pd(1)–Cl(2) arrays are almost linear with the bond angles of 178.5(3) $^{\circ}$ and 176.3(4) $^{\circ}$. The bond distances of Pd(1)–C(10), Pd(1)–Cl(1) and Pd(1)–N(5) are 1.926(6) Å, 2.325(1) Å and 2.081(6) Å, respectively.

It has been known that the α -hydrogen atoms of acetonitrile can be deprotonated one by one in the presence of base to form singly, doubly and triply deprotonated acetonitrile (i.e., [CH₂CN][−] [52–55], [CHCN]^{2−} [56,57] and [CCN]^{3−} [45,58,59]). The different formulae of deprotonated acetonitriles could be relative to the amount of base and the type of coordinated metal ions in the system of reaction. The α -carbon atoms of these deprotonated acetonitrile along with other ligands are coordinated to metal ions to form different metal complexes.

In the formation of complex **8**, two α -hydrogen atoms of acetonitrile are deprotonated by strong base KO^tBu to afford a doubly deprotonated acetonitrile (CHCN^{2−}). Then the doubly deprotonated acetonitrile and a bidentate dicarbene ligand coordinate with two Hg(II) atoms to form a funnel-like complex **8** as

shown in Fig. 5(a). In cation of complex **8**, each mercury atom is surrounded by one carbene carbon atom (C_{carbene}) and one α -carbon (C _{α}) atom of acetonitrile. The C(1)–Hg(2)–C(23) and C(17)–Hg(3)–C(23) are nearly linear with the same bond angle of 175.3(5) $^{\circ}$. The bond distance of Hg–C_{carbene} is 2.068(1) Å, which is similar to those of known carbene mercury(II) complexes [33,60–63]. The distance of Hg–C _{α} is 2.080(1) Å, and it is slightly longer than that of Hg–C_{carbene}. The benzene ring and two imidazole rings form the dihedral angles of 79.0(6) $^{\circ}$ and 89.1(7) $^{\circ}$, respectively. Two imidazole rings form a dihedral angle of 55.6(8) $^{\circ}$. It is noteworthy that the cyanomethyl moiety (C(23)–C(22)–N(5)) is nearly linear with bond angle of 176.4(1) $^{\circ}$. The C(23)–C(22) bond distance (1.414(9) Å) is shorter than that of the regular C–C single bond (1.54–1.59 Å), and it has part double-bond characteristics. The C(22)–N(5) bond distance (1.225(9) Å) is similar to that of other complexes containing cyano groups, and this value is expected for a triple bond with a small amount of double bond characteristics [45,52–59,64].

In complex **9**, each cation contains a 10-membered macro-metallocycle formed by one bidentate chelate carbene ligand and one metal atom (Fig. 6(a)). The mercury(II) atom is tricoordinated with two carbene carbon atoms and one iodine atom. The angles of C(7)–Hg(1)–C(28) and C(7)–Hg(1)–I(1) are 158.9(4) $^{\circ}$ and 100.7(3) $^{\circ}$, and the distances of Hg(1)–C(7) and Hg(1)–I(1) are 2.098(9) Å and 2.927(1) Å. These data are analogous to those of some known NHC mercury(II) complexes [33–35]. The structure of [HgI₄]^{2−} in **9** is similar to that of the same unit in **5**.

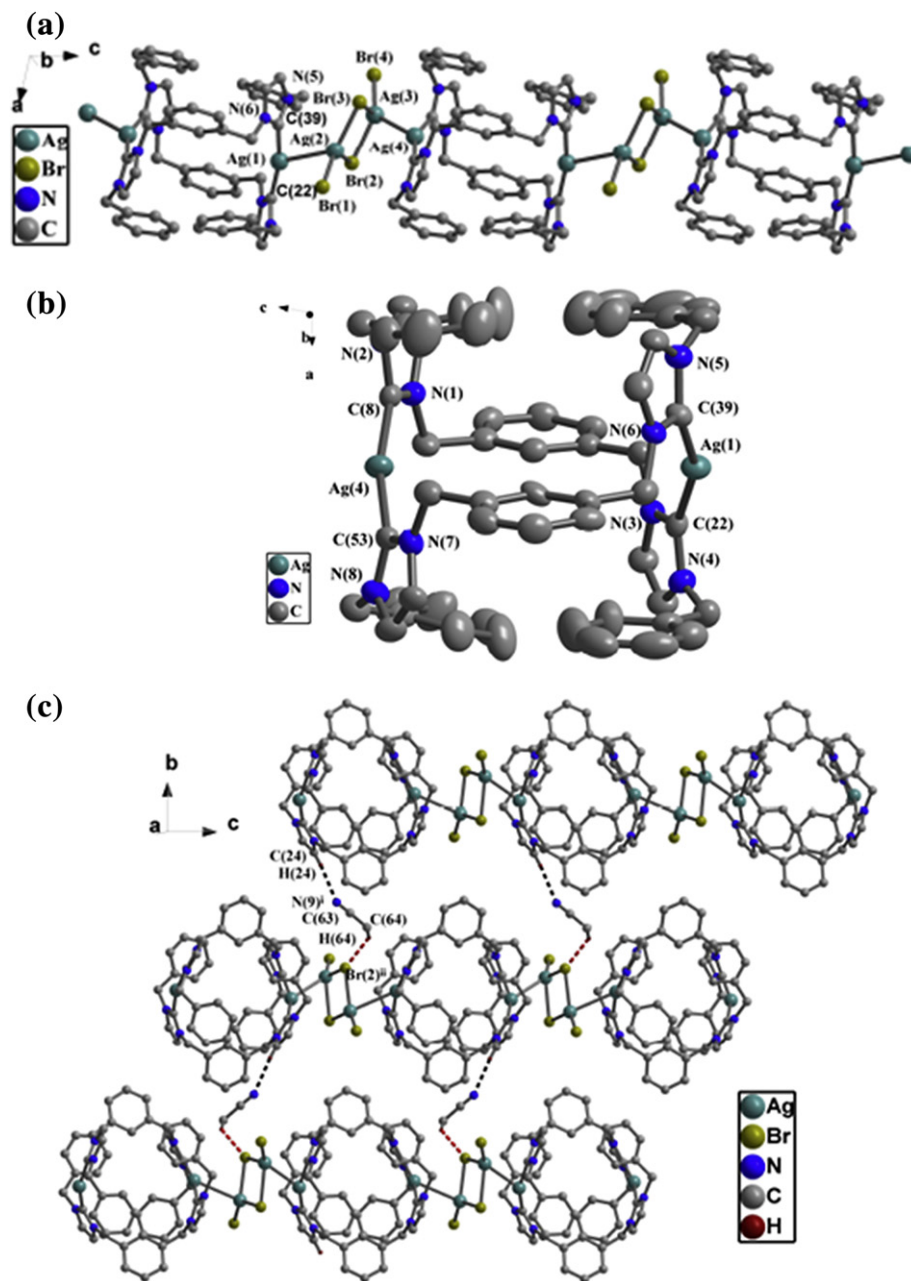


Fig. 3. (a). The 1D polymeric chain of **6**. All hydrogen atoms and methyl groups on mesitylene were omitted for clarity. Selected bond lengths (Å) and angles ($^{\circ}$): Ag(1)–Ag(2) 2.997(6), Ag(2)–Br(1) 2.548(8), Ag(2)–Br(2) 2.620(9), Ag(2)–Br(3) 2.802(8); C(22)–Ag(1)–Ag(2) 139.8(1), C(39)–Ag(1)–Ag(2) 61.9(1), Ag(2)–Br(2)–Ag(3) 82.7(3), Br(1)–Ag(2)–Br(2) 129.1(3), N(5)–C(39)–N(6) 104.5(4). (b). Perspective view of the cage-like in the cation of **6**. All hydrogen atoms and methyl groups on mesitylene were omitted for clarity. Selected bond lengths (Å) and angles ($^{\circ}$): Ag(1)–C(22) 2.105(6), Ag(1)–C(39) 2.116(6); C(22)–Ag(1)–C(39) 156.5(2), N(3)–C(22)–N(4) 104.6(5). (c). 2D supramolecular layer of **6** via C–H \cdots N and C–H \cdots Br hydrogen bonds. All hydrogen atoms except those participating in the hydrogen bonds and all methyl groups on mesitylene were omitted for clarity.

2.4. The crystal packings of precursor **2** and complexes **5–9**

Some weak interactions, including classical hydrogen bonds (such as Y–H \cdots X hydrogen bonds, Y or X = F, N, O), nonclassical hydrogen bonds (such as C–H \cdots A hydrogen bonds, A = O, N, F, Cl, Br, I and π , etc.) and aromatic π – π interactions play important roles in crystal packings, and they can further link discrete subunits or low-dimensional entities into high-dimensional supramolecular networks [65,66]. The results of theoretical and experimental investigations show that these weak interactions exist widely in the bio-systems and organic crystals [67–69]. Moreover, these weak interactions may result in a collective contribution to the formation

of supramolecular architecture. In the nonclassical hydrogen bonds C–H \cdots A, the H \cdots A distance is different due to the difference of A. Generally, when H \cdots A distance is less than the sum of van der Waals radii of H and A, C–H \cdots A interactions should be considered (the sum of van der Waals radii for hydrogen atom and A atom (Å): H and F = 2.67, H and I = 3.35, H and N = 2.70, H and Br = 3.15). For example, the Steiner put forward that C–H \cdots O interactions may exist when H \cdots O distance is less than 2.7 Å [70]. Tiekink believed that the C–H \cdots π contacts should be considered when H \cdots π distance is within 2.4–3.6 Å [71]. Whereas, the π – π interactions of aromatic rings should be considered when face-to-face distance is about 3.5 Å [72].

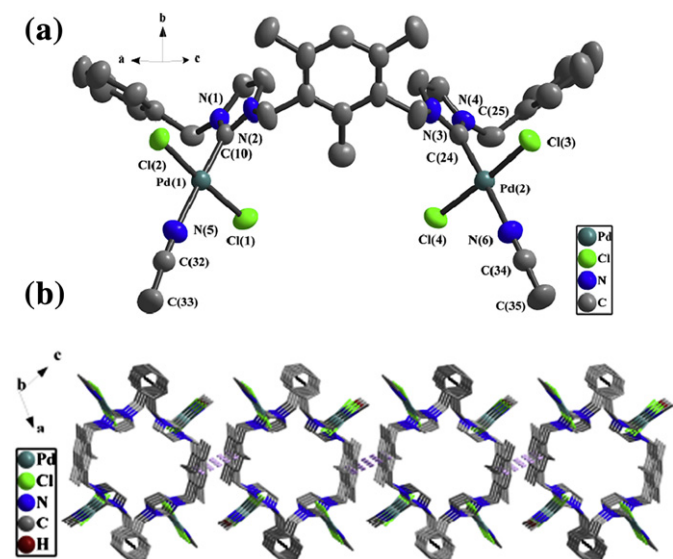


Fig. 4. (a). Perspective view of **7** and anisotropic displacement parameters depicting 50% probability. All hydrogen atoms were omitted for clarity. Selected bond lengths (Å) and angles (°): Pd(1)–C(10) 1.928(6), Pd(1)–N(5) 2.081(6), Pd(1)–Cl(1) 2.330(1); C(10)–Pd(1)–N(5) 178.5(2), C(10)–Pd(1)–Cl(2) 89.2(1), C(10)–Pd(1)–Cl(1) 88.2(1), Cl(2)–Pd(1)–Cl(1) 176.2 (7), N(1)–C(10)–N(2) 105.0(5), C(32)–N(5)–Pd(1) 172.9(6). (b). 2D supramolecular layer of **7** via two types of π – π interactions. All hydrogen atoms were omitted for clarity.

1D supramolecular chain of **2** (Fig. 1(b)) is formed via C–H \cdots F hydrogen bonds (the data of hydrogen bonds being given in Table 2). In the hydrogen bonds, hydrogen atoms are from imidazole rings and methyl groups of mesitylene, respectively. These values of hydrogen bonds are comparable with analogous those reported [51].

As shown in Fig. 2(b), 2D supramolecular layer of **5** is formed via C–H \cdots I hydrogen bonds (Table 2), and the hydrogen atoms in these hydrogen bonds are from benzimidazole ring and benzene ring of benzyl groups, respectively. These values of hydrogen bonds are similar to those of literature [73].

In crystal packing of complex **6** (Fig. 3(c)), the adjacent 1D polymeric chains are linked together by free bridging acetonitrile molecules via C–H \cdots Br [74] and C–H \cdots N [75] hydrogen bonds to form 2D supramolecular layers. The hydrogen atoms in C–H \cdots Br hydrogen bonds are from the methyl of acetonitrile, and the hydrogen atoms in C–H \cdots N hydrogen bonds are from the imidazole rings (Table 2). These values of hydrogen bonds are consistent with those published.

Analysis of crystal packing of complex **7** (Fig. 4(b)) reveals that 1D supramolecular tubular structure is formed by two row molecules through π – π interactions from the benzene rings of benzyl

Table 1

Dihedral angles (°) between two imidazole (or benzimidazole) rings (A) on the same ligand, dihedral angles (°) between the mesitylene plane and two imidazole (or benzimidazole) rings on the same ligand (B), and dihedral angles between imidazole (or benzimidazole) ring and adjacent benzene ring of benzyl group (or pyridine ring) (C) for precursor **2** and complexes **5–9**.

Compounds	A	B	C
2	14.3	85.3, 86.0	–
5	21.9	75.6, 80.2	68.8, 88.4
6	51.3	88.9, 81.6	83.6, 88.0
7	86.7	84.2, 88.1	83.8, 84.1
8	55.6	79.0, 89.1	–
9	21.7	76.5, 76.9	–

Table 2

H-Bonding geometry (Å, °) for precursor **2** and complexes **5, 6, 8** and **9**.

	D–H \cdots A	D–H	H \cdots A	D \cdots A	D–H \cdots A
2	C(13)–H(13) \cdots F(2)	0.96(1)	2.655(2)	3.575(2)	160.8(9)
	C(5)–H(5) \cdots F(4)	0.93(1)	2.422(2)	3.324(3)	163.6(9)
5	C(14)–H(14) \cdots I(4)	0.93(1)	2.661(2)	3.495(3)	149.7(1)
	C(4)–H(4) \cdots I(1) ⁱ	0.93(1)	2.900(4)	3.700(4)	144.9(8)
6	C(10)–H(10) \cdots I(1)	0.93(1)	2.998(3)	3.787(5)	143.7(1)
	C(24)–H(24) \cdots N(9) ⁱ	0.93(1)	2.616(3)	3.544(4)	175.8(1)
8	C(64)–H(64) \cdots Br(2) ⁱⁱ	0.96(1)	2.888(2)	3.684(3)	141.0(1)
	C(18)–H(18) \cdots I(4) ⁱ	0.93(1)	3.118(1)	3.961(1)	151.7(1)
9	C(52)–H(52) \cdots I(1) ⁱ	0.97(1)	3.058(1)	3.823(1)	136.6(1)
	C(5)–H(5) \cdots I(5)	0.93(1)	3.145(1)	4.025(1)	158.6(1)
	C(42)–H(42) \cdots I(4)	0.97(1)	3.147(1)	3.897(1)	135.1(1)

Symmetry code: i: 0.5–x, –0.5+y, 1.5–z for **5**; i: 1–x, 0.5+y, –z; ii: 2–x, 0.5+y, –z for **6**; i: –x, –y, –z for **8**; i: –x, 1–y, 1–z for **9**.

groups with the intermolecular separation of 3.501(1) Å. In the 1D tubular structure, the size of cavity is ca. 5.2 \times 10.2 Å². Additionally, 1D tubular chains are further extended into 2D supramolecular layers via another type of π – π interactions from benzene rings of mesitylenes with intermolecular separation of 3.420(2) Å. These values of π – π interactions are fall in the normal ranges [72,76–78].

In the crystal packing of **8** (Fig. 5(b)), 2D supramolecular layer is formed via weak Hg \cdots N bonds (the nitrogen atom being from acetonitrile, the Hg \cdots N distance being 2.859(1) Å, and the sum of van der Waals radii for mercury and nitrogen being 3.2 Å) and C–H \cdots π contacts (H \cdots π distance being 3.050(4) Å, and C–H \cdots π angle being 148.9(1)°). In C–H \cdots π contacts, the hydrogen atoms are from CH₃ of ethyl and π systems are from imidazole rings. These values of C–H \cdots π contacts are within the normal ranges [71,79–81]. Additionally, the anionic unit [HgI₄]^{2–} is packed between successive 2D supramolecular layers and hold layers together via weak Hg \cdots I bonds (the Hg \cdots I distance being 2.788(1) Å, and the sum of van der Waals radii for mercury and iodine being 3.8 Å) and C–H \cdots I hydrogen bonds to form 3D supramolecular frameworks as shown in Fig. 5(c). In C–H \cdots I hydrogen bonds, the iodine atoms are from the anionic unit [HgI₄]^{2–}, and the hydrogen atoms are from imidazole rings. These values of hydrogen bonds are comparable with those reported [73].

In the crystal packing of **9**, 1D double-strand supramolecular chain is formed by C–H \cdots I hydrogen bonds [73] and C–H \cdots π contacts [71,79–81] (Fig. 6(b)). In C–H \cdots I hydrogen bonds, the iodine atoms are from the cations, and the hydrogen atoms are from CH₂ (Table 2). In C–H \cdots π contacts (H \cdots π distance being 3.044(4) Å, and C–H \cdots π angle being 146.1°), the hydrogen atoms are from CH₃ of propyl and π systems are from benzimidazole rings. Additionally, the anionic unit [HgI₄]^{2–} are packed between successive 1D supramolecular chains and hold chains together via two new C–H \cdots I hydrogen bonds to form 2D supramolecular layer (Fig. 6(c)). In new C–H \cdots I hydrogen bonds, the iodine atoms are from the anionic unit [HgI₄]^{2–}, and the hydrogen atoms are from CH₃ and benzimidazole rings, respectively. These values of C–H \cdots I hydrogen bonds and C–H \cdots π contacts are fall in normal ranges.

2.5. The conformations of the diimidazolium (or dibenzimidazolium) salts and their metal complexes

As shown in Scheme 4, the diimidazolium (or dibenzimidazolium) salts with mesitylene linker adopt two diverse conformations (i.e., *cis*-conformation **I** and *trans*-conformation **II**) according to the different arrangements of two Rimi (or Rbimi) arms. The conformations **I** and **II** can converse to each other in the solution, and their ratio may be mostly relative to two factors: (1) the weak interactions between anions and two Rimi (or Rbimi) arms; (2) the

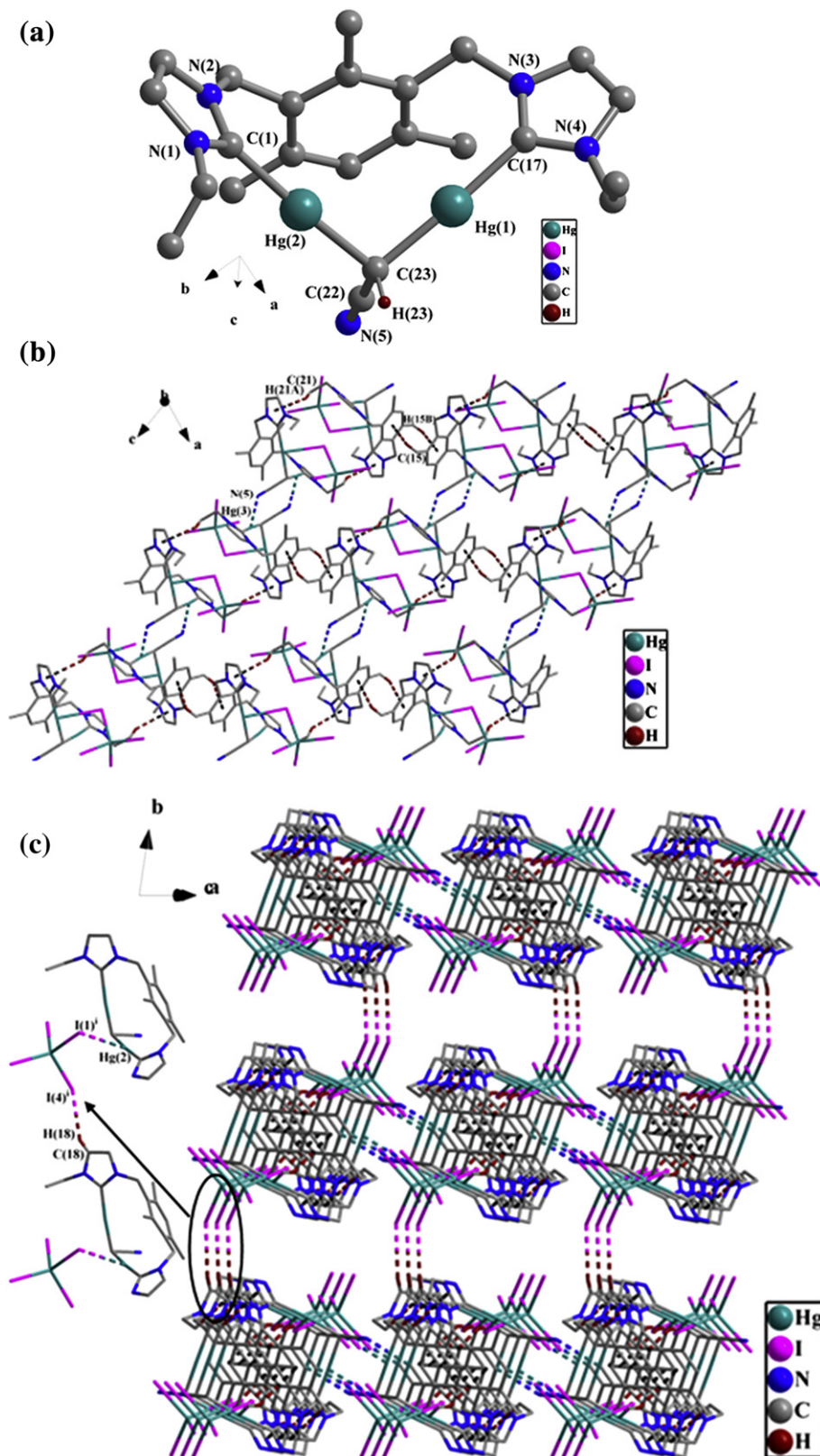


Fig. 5. (a). Perspective view of **8** and anisotropic displacement parameters depicting 50% probability. All hydrogen atoms except that in CHCN were omitted for clarity. Selected bond lengths (Å) and angles ($^{\circ}$): Hg(1)–C(17) 2.070(1), Hg(2)–C(1) 2.068(1), Hg(1)–C(23) 2.080(1), Hg(2)–C(23) 2.092(1); C(1)–Hg(2)–C(23) 175.3(5), C(17)–Hg(3)–C(23) 175.3(4), N(1)–C(1)–N(2) 105.8(1). (b). 2D supramolecular layer of complex **8** via both C–H \cdots π contacts and Hg \cdots N interactions. All hydrogen atoms except those participating in the C–H \cdots π hydrogen bonds were omitted for clarity. (c). 3D supramolecular network of complex **8** via C–H \cdots π contacts, Hg \cdots N interactions and C–H \cdots I hydrogen bonds. All hydrogen atoms except those participating in the C–H \cdots π contacts and C–H \cdots I hydrogen bonds were omitted for clarity.

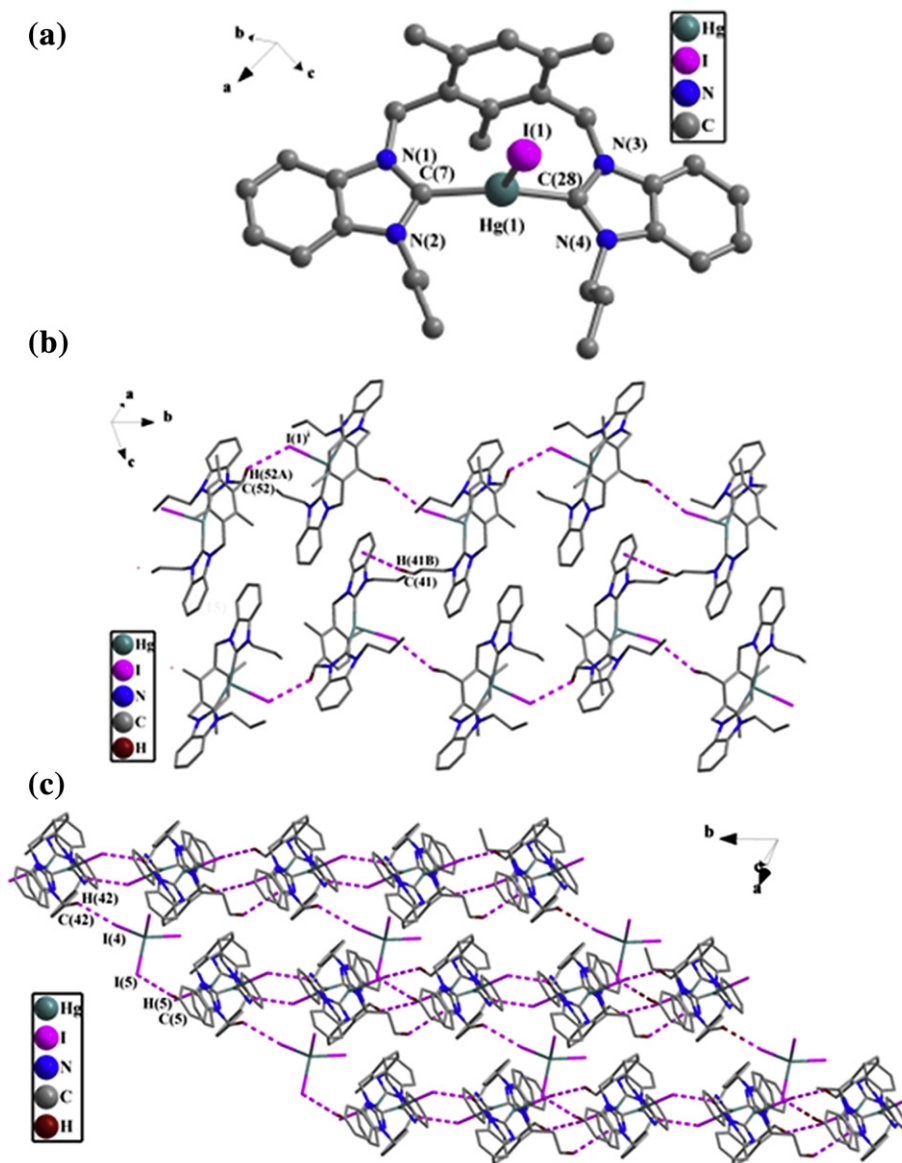


Fig. 6. (a). Perspective view of **9** and anisotropic displacement parameters depicting 50% probability. All hydrogen atoms were omitted for clarity. Selected bond lengths (Å) and angles ($^{\circ}$): Hg(1)–C(7) 2.098(9), Hg(1)–C(28) 2.100(9), Hg(1)–I(1) 2.927(1); C(7)–Hg(1)–C(28) 158.9(4), C(7)–Hg(1)–I(1) 100.7(3), C(28)–Hg(1)–I(1) 100.2(3), N(1)–C(7)–N(2) 108.4(8). (b). 1D double-strand supramolecular chain of **9** by C–H \cdots I hydrogen bonds and C–H \cdots π contacts. All hydrogen atoms except those participating in the C–H \cdots I hydrogen bonds and C–H \cdots π contacts were omitted for clarity. (c). 2D supramolecular layer of **9** by C–H \cdots I hydrogen bonds and C–H \cdots π contacts. All hydrogen atoms except those participating in the C–H \cdots I hydrogen bonds and C–H \cdots π contacts were omitted for clarity.

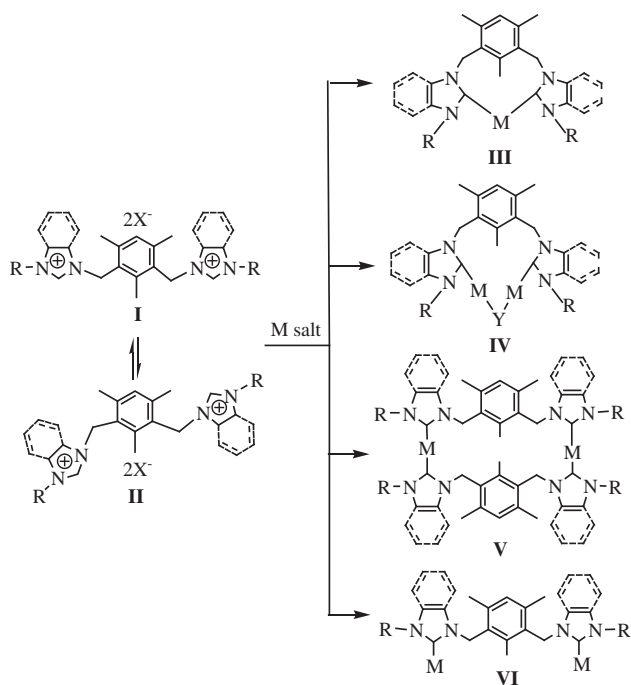
steric hindrance between two Rimi (or Rbimi) arms. The former may have larger effect on the ratio of conformation than the latter. When there exist strong interactions between one anion and two Rimi (or Rbimi) arms at the same time in a compound, the two arms lie in the same side of mesitylene plane, and the compound adopts mainly *cis*-conformation (e.g., **5**). When there exist strong interactions between one anion and only one Rimi (or Rbimi) arm in a compound, two arms lie in the opposite sides of mesitylene plane due to steric hindrance, and thus *trans*-conformation is predominant (e.g., **2**).

NHC metal complexes **6–9** possess four different conformations, namely, the monometal monoligand macrocycle **III** (e.g., **9**), the dimetal monoligand macrocycle **IV** (e.g., **8**), the dimetal diligand macrocycle **V** (e.g., **6**) and the open structure composed of one bidentate dicarbene ligand and two metal atoms **VI** (e.g., **7**). The conformations of the complexes may be relative to the

corresponding precursors' conformations, metal ions, counterions, steric hindrance.

2.6. Catalytic activity of NHC palladium(II) complex **7**

The Suzuki–Miyaura cross-coupling reaction of aryl halides and arylboronic acids is of general interest to organic synthesis. The Suzuki–Miyaura reaction catalyzed by Pd–NHC complexes has been one of the most important methods for the synthesis of unsymmetrically substituted biaryl compounds [46–48]. We choose the cross-coupling reaction of 4-bromotoluene with phenylboronic acid as a model reaction to investigate the solvent and base effects (Table 3). Using absolute MeOH as solvent and KOH as base gives 96% coupling yield at 60 $^{\circ}$ C in 8 h (entry 2). Coupling yield drops to 78%, however, when changing solvent to pure water (entry 3). A mixed solvent of MeOH/H₂O (5:1) in the presence of base KOH gives



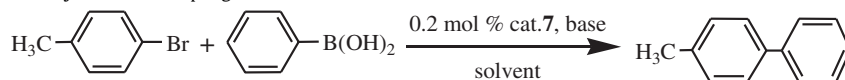
Scheme 4. The diverse conformations of diimidazolium (or dibenzimidazolium) salts and their metal complexes.

yield of 99% in 8 h (entry 11). The higher activity is attributed to the better solubility of catalyst and KOH in the aqueous MeOH mixture and rapid reduction of Pd(II) to Pd(0) [82,83]. Solvents such as dichloromethane, dioxane and acetonitrile afford the product with

moderate to good yields (entries 5, 7 and 8). Other solvents like THF and DMF give poor yields (entries 4 and 6). The common and less expensive inorganic bases, such as $K_3PO_4 \cdot 3H_2O$, K_2CO_3 , Na_2CO_3 and $NaHCO_3$ give high yields in mixed solvent MeOH/ H_2O (5:1) (entries 15, 16, 19 and 20), and they may be prior reagents of choice. NaOAc and $BaCO_3$ give 81% and 50% yields, respectively (entries 18 and 22). Poor yields are obtained using KBr and $Ba(OH)_2$ as base (entries 17 and 21). Based on the extensive screen, MeOH/ H_2O (5:1) and KOH are found to be the most efficient solvent and base with a catalyst loading of 0.2 mol % complex **7** at 60 °C in air, thus giving the optimal coupling result. The reactions were monitored by GC analysis after the appropriate intervals. In order to further study the influence of ligand on catalysis, the control experiment was performed, in which $PdCl_2(CH_3CN)_2$ were added in the absence of ligand with the optimized conditions, and only 25% coupling product was observed (entry 23). This result shows that the ligand has the preponderant function in the catalytic reaction.

We attempted the cross-coupling reactions of various aryl halides with phenylboronic acid under the optimal reaction condition. In general, complex **7** can catalyze the cross-coupling of various aryl halides with phenylboronic acid to give different yields (Table 4). The catalyst is efficient toward the coupling of 4-bromoanisole or 1-bromonaphthalene with phenylboronic acid to give yields of 96% and 90%, respectively (entries 1 and 5). The coupling of 4-nitrobromobenzene or 4-bromoacetophenone with phenylboronic acid leads to moderate yields of 78% and 82%, respectively (entries 3 and 4). The catalyst is highly efficient toward the coupling of iodobenzene with phenylboronic acid to give a near quantitative yield (entry 6). The catalyst is also effective toward the coupling of aryl chlorides with phenylboronic acid. The coupling reaction of 4-nitrochlorobenzene with phenylboronic acid gave moderate yield of 64% (entry 9), while 2-chlorotoluene, 4-chloroaniline, 2,4-

Table 3
Effect of solvent and base on Suzuki–Miyaura cross-coupling Reaction^a.



Entry	Solvent	Base	Time (h) ^b	Yield(%) ^c
1	MeOH	KOH	6	94
2	MeOH	KOH	8	96
3	H ₂ O	KOH	8	78
4	THF	KOH	24	9
5	CH ₂ Cl ₂	KOH	8	53
6	DMF	KOH	8	10
7	dioxane	KOH	8	56
8	CH ₃ CN	KOH	8	84
9	MeOH/ H_2O (2:1)	KOH	8	77
10	MeOH/ H_2O (5:1)	KOH	6	95
11	MeOH/ H_2O (5:1)	KOH	8	99
12	MeOH	$K_3PO_4 \cdot 3H_2O$	8	93
13	H ₂ O	$K_3PO_4 \cdot 3H_2O$	8	46
14	THF	$K_3PO_4 \cdot 3H_2O$	8	18
15	MeOH/ H_2O (5:1)	$K_3PO_4 \cdot 3H_2O$	8	95
16	MeOH/ H_2O (5:1)	K_2CO_3	12	96
17	MeOH/ H_2O (5:1)	KBr	8	24
18	MeOH/ H_2O (5:1)	NaOAc	12	81
19	MeOH/ H_2O (5:1)	Na_2CO_3	12	94
20	MeOH/ H_2O (5:1)	$NaHCO_3$	12	92
21 ^d	MeOH/ H_2O (5:1)	$Ba(OH)_2$	12	16
22 ^d	MeOH/ H_2O (5:1)	$BaCO_3$	8	50
23 ^e	MeOH/ H_2O (5:1)	KOH	8	25

^a Reaction conditions: bromobenzene 0.50 mmol, phenylboronic acid 0.60 mmol, base 1.2 mmol, complex **7** 0.2 mol%, solvent 3 mL, 60 °C in air.

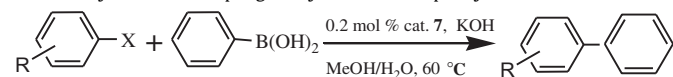
^b Reactions were monitored by TLC.

^c Determined by GC.

^d Complex **7**: 0.4 mol%.

^e Reaction conditions are the same as [a], and only $PdCl_2(CH_3CN)_2$ was added in the absence of ligand.

Table 4
Suzuki–Miyaura cross-coupling of aryl halides with phenylboronic acid^a.



Entry	Aryl halide	Time (h) ^b	Yield (%)
1	4-bromoanisole	8	96 ^c
2 ^d	4-bromoaniline	24	35 ^e
3	4-nitrobromobenzene	24	78 ^e
4	4-bromoacetophenone	24	82 ^e
5	1-bromonaphthalene	12	90 ^e
6	iodobenzene	6	99 ^e
7 ^d	2-chlorotoluene	24	22 ^e
8 ^d	4-chloroaniline	36	23 ^e
9 ^d	4-nitrochlorobenzene	26	64 ^e
10 ^d	2,4-dinitrochlorobenzene	24	24 ^e
11 ^d	2-chloropyridine	24	38 ^e

^a Reaction conditions: Aryl halides 0.50 mmol, phenylboronic acid 0.60 mmol, base 1.2 mmol, complex **7** 0.2 mol%, MeOH/H₂O (5:1) mixed solvent 3 mL, 60 °C in air.

^b Reactions were monitored by TLC.

^c Determined by GC.

^d Complex **7**: 0.4 mol%.

^e Isolated yield.

dinitrochlorobenzene or 2-chloropyridine gave relatively poor yields of 22%–38% (entries 7, 8, 10 and 11). This catalytic system shows good tolerance toward a wide range of sensitive functional groups. Therefore, this provides an alternative and effective phosphine-free catalytic system for facile coupling of aryl halides under mild and aerobic conditions.

According to literature report, the catalytic activity of bi-palladium(II) complexes could be improved by the cooperative effect of two metal centers [84–86]. By comparison, we can see that the catalytic activity of bi–Pd(II) complex **2** in most Suzuki–Miyaura reactions is similar to those of known NHC mono–Pd(II) complexes [87–89]. This catalyst has not shown the outstanding superiority, and the reason could be that the distance between two palladium centers is somewhat far away not to generate effective cooperative interaction. The distance between two metal centers may be an important factor for influence on cooperative interaction. Only a suitable distance between two metal centers can an effective cooperative interaction be generated. Besides, the steric hindrance of around Pd and the structure of different bridging linkers may also have some influence on the activity of catalyst.

2.7. Fluorescent emission spectra of precursors **1** and **3**, and complexes **6** and **9**

As shown in Fig. 7, the fluorescent emission spectra of precursors **1** and **3**, and complexes **6** and **9** in acetonitrile at room temperature are obtained upon excitation at 250 nm (the fluorescent emission spectrum of **2** is similar to that of **1**; the fluorescent emission spectra of **4** and **5** are similar to that of **3**; the fluorescent emission spectra of **7** and **8** are similar to that of **6**). Precursors **1** and **3** exhibit broad emission bands in the region of 325–345 nm, corresponding to intraligand transitions [90]. Complexes **6** and **9** exhibit double emission bands, and the intense emission bands in the region of 325–345 nm are similar to those of corresponding precursors, which should originate from the metal perturbed intraligand processes [91]. It is notable that new emission bands of **6** and **9** in the region of 298–315 nm are observed, which may arise from the electronic transitions of the benzene ring due to the influence of metal and ligand coordination interactions [91–93]. The results show that these metal complexes might have potential application in photoactive materials.

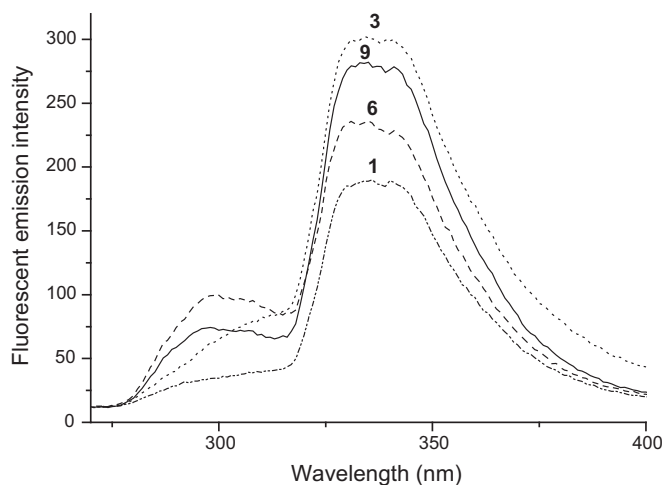


Fig. 7. Emission spectra of **1** (---), **3** (···), **6** (—) and **9** (— · —) at 298 K in CH₃CN (5.0 × 10^{−6} M) solution.

3. Conclusions

In summary, a series of new NHC silver(I), palladium(II) and mercury(II) complexes with mesitylene linker have been synthesized and characterized. The diimidazolium (or dibenzimidazolium) salts adopt two diverse conformations (cis- and trans-conformations), and their NHC metal complexes possess four different conformations. In crystal packings of precursor **2** and complexes **5–9**, 1D supramolecular chains, 2D supramolecular layers or 3D architectures are formed via intermolecular weak interactions, including π – π interactions, hydrogen bonds, C–H \cdots π contacts, and weak Hg \cdots N and Hg \cdots I bonds. NHC palladium(II) complex **7** can catalyze the most Suzuki–Miyaura reaction of aryl halides (iodide, bromide and chloride) with phenylboronic acid using MeOH/H₂O as solvent and KOH as base in air. Further studies on new organometallic compounds from precursors **1–4** and analogous ligands are underway.

4. Experimental section

4.1. General procedures

All manipulations were performed using Schlenk techniques, and solvents were purified by standard procedures. All the reagents for synthesis and analyses were of analytical grade and used without further purification. Melting points were determined with a Boetius Block apparatus. ¹H and ¹³C NMR spectra were recorded on a Varian Mercury Vx 400 spectrometer at 400 MHz and 100 MHz, respectively. Chemical shifts, δ , are reported in ppm relative to the internal standard TMS for both ¹H and ¹³C NMR. *J* values are given in Hz. Elemental analyses were measured using a Perkin–Elmer 2400C Elemental Analyzer. The luminescent spectra were conducted on a Cary Eclipse fluorescence spectrophotometer. GC analysis was carried out using a Focus DSQI GC–MS equipped with an integrator (C-R8A) with a capillary column (CBP-1 or CBP-5, 0.25 mm i.d. × 40 m).

4.2. Synthesis of 1,3-bis[1-benzylimidazolomethyl]mesitylene bromide (**1**)

A THF solution (40 mL) of imidazole (1.420 g, 20.8 mmol) was added to a suspension of oil-free sodium hydride (0.500 g, 20.8 mmol) in THF (40 mL) and stirred for 1 h at 60 °C. Then benzyl

bromide (3.240 g, 19.0 mmol) was added dropwise to the above solution. The mixture was stirred for 22 h at 60 °C, and a brown solution was obtained. The solvent was removed with a rotary evaporator and H₂O (50 mL) was added to the residue. Then the solution was extracted with CH₂Cl₂ (3 × 30 mL), and the extracting solution was dried with anhydrous MgSO₄. After removing CH₂Cl₂, a pale yellow solid was obtained.

A solution of 1-benzylimidazole (2.274 g, 14.4 mmol) and 1,3-dibromomethylmesitylene (2.000 g, 6.5 mmol) in acetone (100 mL) was stirred for five days under refluxing, and a white precipitate was formed. The product was filtered and washed with acetone. The white powder of 1,3-bis[1-benzylimidazolomethyl]mesitylene bromide (**1**) was obtained by recrystallization from methanol/ether. Yield: 3.656 g (90%). M.p.: 278–280 °C. Anal. Calcd for C₃₁H₃₄N₄Br₂: C, 59.82; H, 5.51; N, 9.00%. Found: C, 59.53; H, 5.72; N, 9.41%. ¹H NMR (400 MHz, DMSO-d₆): δ 2.09 (s, 6H, CH₃), 2.31 (s, 3H, CH₃), 5.42 (s, 4H, CH₂), 5.50 (s, 4H, CH₂), 7.19 (s, 1H, PhH), 7.40 (m, 10H, PhH), 7.65 (s, 2H, imiH), 7.85 (s, 2H, imiH), 9.24 (s, 2H, 2-imiH) (imi = imidazole).

4.3. Synthesis of 1,3-bis[1-ethylimidazolomethyl]mesitylene hexafluorophosphate (**2**)

A solution of 1-ethylimidazole (1.382 g, 14.4 mmol) and 1,3-dibromomethylmesitylene (2.000 g, 6.5 mmol) in THF (100 mL) was stirred for five days under refluxing, and a white precipitate was formed. The product was filtered and washed with THF. The white powder of 1,3-bis[1-ethylimidazolomethyl]mesitylene bromide was obtained by recrystallization from methanol/ether. Yield: 3.021 g (93%). M.p.: 258–260 °C.

NH₄PF₆ (1.439 g, 8.8 mmol) was added to a methanol solution of 1,3-bis[1-ethylimidazolomethyl]mesitylene bromide (2.000 g, 4.0 mmol) whilst stirring, and a white precipitate was formed immediately. The product was collected by filtration, washed with small portions of cold methanol, and dried in vacuum to give a white powder of 1,3-bis[1-ethylimidazolomethyl]mesitylene hexafluorophosphate (**2**). Yield: 2.318 g (92%). M.p.: 192–194 °C. Anal. Calcd for C₂₁H₃₀F₁₂N₄P₂: C, 40.14; H, 4.81; N, 8.92%. Found: C, 40.53; H, 4.44; N, 8.64%. ¹H NMR (400 MHz, DMSO-d₆): δ 1.23 (t, J = 3.6, 6H, CH₃), 1.96 (s, 3H, CH₃), 2.13 (s, 6H, CH₃), 3.95 (q, J = 3.6, 4H, CH₂), 5.25 (s, 4H, CH₂), 7.03 (s, 1H, PhH), 7.13 (s, 2H, imiH), 7.30 (s, 2H, imiH), 8.32 (s, 2H, 2-imiH).

The following dibenzimidazolium salts **3** and **4** were prepared in a manner analogous to that of **2**, only instead of ammonium hexafluorophosphate with sodium iodide in the second step.

4.4. Synthesis of 1,3-bis[1-(*n*-propyl)benzimidazolomethyl]mesitylene iodide (**3**)

Yield: 3.693 g (90%). M.p.: 250–252 °C. Anal. Calcd for C₃₁H₃₈N₄I₂: C, 51.68; H, 5.32; N, 7.78%. Found: C, 51.37; H, 5.61; N, 7.92%. ¹H NMR (400 MHz, DMSO-d₆): δ 1.25 (t, J = 6.0, 6H, CH₃), 1.91 (m, 4H, CH₂), 2.09 (s, 6H, CH₃), 2.36 (s, 3H, CH₃), 4.25 (t, J = 5.4, 4H, CH₂), 5.77 (s, 4H, CH₂), 7.32 (s, 1H, PhH), 7.51 (m, 4H, PhH), 7.83 (d, J = 7.4, 2H, PhH), 8.20 (d, J = 7.4, 2H, PhH), 9.62 (s, 2H, 2-bimiH). ¹³C NMR (100 MHz, DMSO-d₆): δ 140.9 and 140.3 (2-bimic), 139.5, 131.6, 131.4, 127.5, 126.8, 126.6, 113.9 and 113.8 (PhC), 48.0 (NCH₂Ph), 45.4 (NCH₂CH₂CH₃), 22.3 (CH₂CH₂CH₃), 19.6 and 15.5 (PhCH₃), 10.5 (CH₂CH₂CH₃) (bimi = benzimidazole).

4.5. Synthesis of 1,3-bis[1-benzylimidazolomethyl]mesitylene iodide (**4**)

Yield: 3.600 g (63%). M.p.: 260–262 °C. Anal. Calcd for C₃₉H₃₈N₄I₂: C, 57.37; H, 4.69; N, 6.86%. Found: C, 57.21; H, 4.84; N, 6.52%. ¹H NMR (400 MHz, DMSO-d₆): δ 2.09 (s, 6H, CH₃), 2.30 (s, 3H,

CH₃), 5.76 (s, 4H, CH₂), 5.79 (s, 4H, CH₂), 7.30 (m, 9H, PhH), 7.42 (d, J = 7.0, 2H, PhH), 7.63 (t, J = 7.0, 2H, PhH), 7.70 (t, J = 6.8, 2H, PhH), 7.88 (d, J = 7.8, 2H, PhH), 8.20 (d, J = 7.8, 2H, PhH), 9.77 (s, 2H, 2-bimiH). ¹³C NMR (100 MHz, DMSO-d₆): δ 141.3 and 140.4 (2-bimic), 134.1, 131.7, 131.1, 128.8, 128.5, 127.8, 127.5, 126.9, 126.7, 114.0 and 113.9 (PhC), 49.8 and 45.6 (NCH₂Ph), 19.6 and 15.7 (PhCH₃).

4.6. Synthesis of [1,3-bis(1-benzylimidazolomethyl)mesitylene][HgI₄] (**5**)

Mercury iodide (0.277 g, 0.6 mmol) was added to a solution of 1,3-bis[1-benzylimidazolomethyl]mesitylene iodide (**6**) (0.200 g, 0.3 mmol) in dichloromethane (30 mL) and the solution was stirred for 24 h under refluxing. The resulting solution was filtered and concentrated to 5 mL, and Et₂O (8 mL) was added to precipitate a pale yellow powder. Isolation by filtration yielded anionic complex **5**. Yield: 0.182 g (52%). M.p.: 284–286 °C. Anal. Calcd for C₃₉H₃₈HgI₄N₄: C, 36.86; H, 3.01; N, 4.41%. Found: C, 36.62; H, 3.45; N, 4.21%. ¹H NMR (400 MHz, DMSO-d₆): δ 2.10 (s, 6H, CH₃), 2.36 (s, 3H, CH₃), 5.81 (s, 4H, CH₂), 5.88 (s, 4H, CH₂), 7.36 (m, 9H, PhH), 7.47 (d, J = 7.2, 2H, PhH), 7.69 (t, J = 7.2, 2H, PhH), 7.78 (t, J = 7.0, 2H, PhH), 7.93 (d, J = 7.4, 2H, PhH), 8.31 (d, J = 7.4, 2H, PhH), 9.85 (s, 2H, 2-bimiH). ¹³C NMR (100 MHz, DMSO-d₆): δ 141.2 and 140.4 (2-bimic), 134.1, 131.7, 131.1, 128.8, 128.5, 127.7, 127.5, 126.9, 126.7, 114.0 and 113.9 (PhC), 49.9 and 45.6 (NCH₂Ph), 19.6 and 15.6 (PhCH₃).

4.7. Synthesis of {[mesitylene(CH₂imyPhCH₂)₂]₂Ag₂·Ag₂Br₄]_n (**6**)

Silver oxide (0.081 g, 0.4 mmol) was added to a solution of 1,3-bis[1-benzylimidazolomethyl]mesitylene bromide (**1**) (0.200 g, 0.3 mmol) in dichloromethane (30 mL) and the suspension solution was stirred for 24 h under refluxing in N₂ protection. The resulting solution was filtered and concentrated to 5 mL, and Et₂O (5 mL) was added to precipitate a white powder. Isolation by filtration yielded complex **6**. Yield: 0.174 g (59%). M.p.: 174–176 °C. Anal. Calcd for C₆₂H₆₄Ag₄Br₄N₈: C, 44.53; H, 3.86; N, 6.70%. Found: C, 44.32; H, 3.64; N, 6.91%. ¹H NMR (400 MHz, DMSO-d₆): δ 2.08 (s, 6H, CH₃), 2.30 (s, 3H, CH₃), 5.35 (s, 4H, CH₂), 5.45 (s, 4H, CH₂), 7.12 (m, 5H, PhH), 7.39 (m, 4H, PhH), 7.64 (m, 4H, PhH or imiH), 7.78 (m, 2H, PhH or imiH). ¹³C NMR (100 MHz, DMSO-d₆): δ 179.3 (C_{carbene}), 139.0, 138.4, 131.9, 131.4, 129.1, 127.6, 123.4, 122.7 and 122.6 (PhC or imiC), 56.1 and 49.9 (NCH₂Ph), 21.0 and 17.5 (PhCH₃).

4.8. Synthesis of {mesitylene[(CH₂imyPhCH₂)PdCl₂(CH₃CN)]₂} (**7**)

The suspension solution of complex **9** (0.668 g, 0.4 mmol) and PdCl₂(CH₃CN)₂ (0.092 g, 0.4 mmol) in dichloromethane (30 mL) was stirred for 24 h under refluxing in N₂ protection. The resulting solution was filtered and concentrated to 5 mL, and Et₂O (5 mL) was added to precipitate a pale yellow powder. Isolation by filtration yielded complex **7**. Yield: 0.167 g (57%). M.p.: 264–266 °C. Anal. Calcd for C₃₅H₃₈Cl₄N₆Pd₂: C, 46.85; H, 4.27; N, 9.37%. Found: C, 46.62; H, 4.53; N, 9.21%. ¹H NMR (400 MHz, DMSO-d₆): δ 2.08 (s, 6H, CH₃), 2.32 (s, 3H, CH₃), 2.35 (s, 6H, CH₃CN), 5.61–5.71 (m, 8H, CH₂), 6.62–6.72 (m, 3H, PhH), 7.10–7.30 (m, 2H, PhH or imiH), 7.32–7.46 (m, 8H, PhH or imiH), 7.56 (d, J = 6.4, 2H, PhH). ¹³C NMR (100 MHz, DMSO-d₆): δ 153.3 (C_{carbene}), 139.8, 136.7, 131.4, 129.2, 129.0, 128.8, 128.6, 123.3 and 121.6 (PhC or imiC), 54.9, 50.1 and 49.9 (NCH₂Ph or CN), 21.3 and 17.6 (PhCH₃ or CH₃CN). IR (KBr): ν CN, 2150 cm⁻¹.

4.9. Synthesis of {mesitylene[(CH₂imyEt)₂Hg₂(CHCN)]₂}[HgI₄] (**8**)

Mercury iodide (0.454 g, 1.0 mmol) was added to a solution of 1,3-bis[1-ethylimidazolomethyl]-2,4,6-trimethylbenzene bromide

(0.200 g, 0.4 mmol) in acetonitrile (30 mL) and the suspension solution was stirred for 24 h at refluxing. The resulting solution was filtered and concentrated to 5 mL, and Et₂O (10 mL) was added to precipitate a yellow powder. Isolation by filtration yielded complex **8**. Yield: 0.260 g (48.3%). M.p.: 176–178 °C. Anal. Calcd for C₂₃H₂₉Hg₃I₄N₅: C, 18.60; H, 1.97; N, 4.72%. Found: C, 18.74; H, 2.06; N, 4.53%. ¹H NMR (400 MHz, DMSO-d₆): δ 1.42 (t, J = 2.6, 6H, CH₃), 2.09 (s, 9H, PhCH₃), 2.37 (s, H, CNCH), 4.25–4.32 (m, 4H, CH₂CH₃), 5.43 (s, 4H, CH₂Ph), 7.81–7.84 (m, 4H, imiH), 7.86 (s, 1H, PhH), (imi = imidazole). IR (KBr): ν CN, 2137 cm⁻¹. ¹³C NMR (100 MHz, DMSO-d₆): δ 180.0 (C_{carbene}), 141.8, 140.7, 133.2, 130.3, 129.3, 125.1, 123.5 and 122.8 (PhC, imiC or CN), 49.6 (NCH₂Ph), 48.1 (NCH₂CH₃), 32.1 (HgCCN), 21.4 and 20.8 (PhCH₃), 17.4 (CH₂CH₃).

4.10. Synthesis of [mesitylene(CH₂bimyⁿPr)₂HgI]_{1/2}[HgI₄] (**9**)

A suspension of KO^tBu (0.112 g, 1.0 mmol), mercury iodide (0.319 g, 0.7 mmol) and 1,3-bis[1-(n-propyl)benzimidazolomethyl] mesitylene iodide (**3**) (0.200 g, 0.3 mmol) in dichloromethane (30 mL) was stirred for 24 h under refluxing in N₂ protection. The resulting solution was filtered and concentrated to 5 mL, and Et₂O (10 mL) was added to precipitate a pale yellow powder. Isolation by filtration yielded complex **9**. Yield: 0.214 g (59%). M.p.: 270–272 °C. Anal. Calcd for C₃₁H₃₆Hg_{1.5}I₃N₄: C, 32.48; H, 3.17; N, 4.89%. Found: C, 32.31; H, 3.45; N, 4.67%. ¹H NMR (400 MHz, DMSO-d₆): δ 0.97 (t, J = 6.2, 6H, CH₃), 2.04 (m, 4H, CH₂), 2.16 (s, 6H, CH₃), 2.62 (s, 3H, CH₃), 4.42 (m, 2H, CH₂), 4.55 (m, 2H, CH₂), 5.73 (d, J = 11.4, 2H, CH₂), 6.10 (d, J = 11.4, 2H, CH₂), 7.33 (s, 1H, PhH), 7.72 (m, 4H, PhH), 8.06 (d, J = 7.0, 2H, PhH), 8.28 (d, J = 7.0, 2H, PhH). ¹³C NMR (100 MHz, DMSO-d₆): δ 184.1 (C_{carbene}), 141.1, 137.9, 134.9, 134.4, 133.7, 129.1, 126.5, 126.2 and 113.4 (PhC), 51.2 (NCH₂Ph), 45.7 (NCH₂CH₂), 31.1, 23.1 and 21.0 (PhCH₃), 17.2 (CCH₂C), 11.4 (CH₂CH₃).

4.11. General procedure for the Suzuki–Miyaura cross-coupling reaction

In a typical reaction, aryl halide (0.5 mmol), phenylboronic acid (0.6 mmol), base (1.2 mmol) and Pd–NHC complex **7** (0.2 mol %) in organic solvent (2.5 mL) and water (0.5 mL if needed) were stirred at 60 °C in air. After the desired reaction time, the reaction was stopped, and water (20 mL) was added to the reaction mixture. The mixture was extracted by n-hexane (10 mL × 3), and the organic layer was washed with water (10 mL × 3) and dried over anhydrous MgSO₄. Then the solution was filtered and concentrated to 5 mL. The solution was analyzed by GC or separated by a column to get the products.

4.12. X-ray structure determinations

For complexes **2**, and **5–9** selected single crystals were mounted on a Bruker APEX II CCD diffractometer at 293(2) K with Mo-Kα radiation (λ = 0.71073 Å) by ω scan mode. Data collection and reduction were performed using the SMART and SAINT software [94] with frames of 0.6° oscillation in the range of 1.8° < φ < 25°. An empirical absorption correction was applied using the SADABS program [95]. The structures were solved by direct methods and all non-hydrogen atoms were subjected to anisotropic refinement by full-matrix least squares on F² using the SHELXTL package [96]. All hydrogen atoms were generated geometrically (C–H bond lengths fixed at 0.96 Å), assigned appropriated isotropic thermal parameters and included in the final calculations. Crystallographic data were summarized in Table 5 and Table 6 for **2** and **5–9**.

Table 5
Summary of crystallographic data for **2**, **5** and **6**.

	2	5	6 ·4CH ₃ CN
Chemical formula	C ₂₁ H ₃₀ F ₁₂ N ₄ P ₂	C ₃₉ H ₃₈ HgI ₄ N ₄	C ₆₂ H ₆₄ Ag ₄ Br ₄ N ₈ ·4CH ₃ CN
fw	628.43	1270.92	1836.55
Cryst syst	Triclinic	Monoclinic	Monoclinic
space group	Pī	P2 ₁ /n	P2 ₁ /n
a/Å	8.973(9)	11.519(1)	10.869(1)
b/Å	10.305(1)	22.071(3)	24.594(3)
c/Å	15.828(1)	16.697(2)	13.847(1)
α/deg	97.7(1)	90	90
β/deg	105.1(2)	106.0(2)	100.2(2)
γ/deg	96.6(2)	90	90
V/Å ³	1381.9(2)	4080.1(9)	3641.6(8)
Z	2	4	2
D _{calcd} , Mg/m ³	1.510	2.069	1.675
Abs coeff, mm ⁻¹	0.257	6.830	3.302
F(000)	644	2368	1816
Cryst size, mm	0.32 × 0.30 × 0.22	0.32 × 0.30 × 0.20	0.38 × 0.32 × 0.28
θ _{min} , θ _{max} , deg	1.35, 25.03	1.85, 25.03	1.49, 25.03
T/K	296(2)	296(2)	296(2)
No. of data collected	7114	20364	18688
No. of unique data	4851	7176	12415
No. of refined params	356	436	819
Goodness-of-fit on F ^{2a}	1.055	1.023	1.025
Final R indices ^b [I > 2σ(I)]			
R ₁	0.0731	0.0766	0.0380
wR ₂	0.2089	0.2286	0.0775
R indices (all data)			
R ₁	0.0850	0.1091	0.0554
wR ₂	0.2239	0.2664	0.0841

^a Goof = [Σω(F_o² - F_c²)/(n - p)]^{1/2}, where n is the number of reflection and p is the number of parameters refined.

^b R₁ = Σ(|F_o - F_c|)/Σ|F_o|; wR₂ = [Σ[w(F_o² - F_c²)]/Σw(F_o²)]^{1/2}.

Table 6
Summary of crystallographic data for **7–9**.

	7 ·H ₂ O	8	9
chemical formula	C ₃₅ H ₃₈ Cl ₄ N ₆ Pd ₂ ·H ₂ O	C ₂₃ H ₂₉ Hg ₃ I ₄ N ₅	C ₃₁ H ₃₆ Hg _{1.5} I ₃ N ₄
fw	915.33	1484.88	1146.23
Cryst syst	Monoclinic	Triclinic	Triclinic
Space group	P2 ₁ /n	Pī	Pī
a/Å	18.896(1)	11.665(1)	13.262(3)
b/Å	8.818(6)	13.163(2)	16.872(4)
c/Å	26.377(1)	13.284(2)	17.247(4)
α/deg	90	81.8(3)	70.8(4)
β/deg	110.3(1)	68.1(3)	89.1(3)
γ/deg	90	84.4(3)	73.3(3)
V/Å ³	4121.4(5)	1872.0(5)	3480.2(1)
Z	4	2	2
D _{calcd} , Mg/m ³	1.475	2.634	2.187
Abs coeff, mm ⁻¹	1.166	15.588	9.304
F(000)	1840	1308	2114
Cryst size, mm	0.38 × 0.32 × 0.30	0.22 × 0.20 × 0.18	0.22 × 0.20 × 0.18
θ _{min} , θ _{max} , deg	1.16, 25.03	2.01, 25.01	1.61, 25.01
T/K	296(2)	296(2)	296(2)
No. of data collected	20400	9494	17576
No. of unique data	7298	6481	12119
No. of refined params	457	321	780
Goodness-of-fit on F ^{2a}	1.078	1.061	1.033
Final R indices ^b [I > 2σ(I)]			
R ₁	0.0509	0.0568	0.0458
wR ₂	0.1735	0.1494	0.1067
R indices (all data)			
R ₁	0.0681	0.0690	0.0862
wR ₂	0.1928	0.1580	0.1241

^a Goof = [Σω(F_o² - F_c²)/(n - p)]^{1/2}, where n is the number of reflection and p is the number of parameters refined.

^b R₁ = Σ(|F_o - F_c|)/Σ|F_o|; wR₂ = [Σ[w(F_o² - F_c²)]/Σw(F_o²)]^{1/2}.

Acknowledgments

This work was financially supported by the National Natural Science Foundation of China (No. 21172172), Tianjin Natural Science Foundation (No. 11JCZDJC22000) and the Open Foundation of State Key Laboratory of Elemento-organic Chemistry, Nankai University (No. 201203).

Appendix A. Supplementary material

CCDC 794741, 794739, 794740, 794734, 891372 and 794735 contain the supplementary crystallographic data for **2** and **5–9** respectively. These data can be obtained free of charge via <http://www.ccdc.cam.ac.uk/conts/retrieving.html>, or from the Cambridge Crystallographic Data Centre, 12 Union Road, Cambridge, CB2 1EZ, UK; fax: (+44) 1223-336-033; or e-mail: deposit@ccdc.cam.ac.uk.

Appendix B. Supporting information

Supporting information related to this article can be found at <http://dx.doi.org/10.1016/j.jorganchem.2013.01.026>.

References

- [1] P.L. Arnold, I.J. Casely, *Chem. Rev.* 109 (2009) 3599–3611.
- [2] F.E. Hahn, M.C. Jahnke, *Angew. Chem. Int. Ed.* 47 (2008) 3122–3172.
- [3] X. Wang, S. Liu, L.H. Weng, G.X. Jin, *Organometallics* 23 (2004) 6002–6007.
- [4] B. Liu, Q. Xia, W. Chen, *Angew. Chem. Int. Ed.* 48 (2009) 5513–5515.
- [5] G.C. Vougioukalakis, R.H. Grubbs, *Chem. Rev.* 110 (2010) 1746–1787.
- [6] C. Samojowicz, M. Bieniek, K. Grela, *Chem. Rev.* 109 (2009) 3708–3742.
- [7] F.E. Hahn, M.C. Jahnke, T. Pape, *Organometallics* 26 (2007) 150–154.
- [8] S.C. Zinner, C.F. Rentsch, E. Herdtweck, W.A. Herrmann, F.E. Kühn, *Dalton Trans.* 35 (2009) 7055–7062.
- [9] B. Liu, D. Xu, W. Chen, *Chem. Commun.* 47 (2011) 2833–2836.
- [10] M.V. Baker, D.H. Brown, R.A. Haque, B.W. Skelton, A.H. White, *J. Incl. Phenom. Macrocycl. Chem.* 65 (2009) 97–109.
- [11] G. Anantharaman, K. Elango, *Synth. React. Inorg. Met.–Org. Nano-Metal Chem.* 37 (2007) 719–723.
- [12] E. Alcalde, R.M. Ceder, C. López, N. Mesquida, G. Muller, S. Rodríguez, *Dalton Trans.* 25 (2007) 2696–2706.
- [13] S.K. Schneider, J. Schwarz, G.D. Frey, E. Herdtweck, W.A. Herrmann, *J. Organomet. Chem.* 692 (2007) 4560–4568.
- [14] M. Raynal, C.S.J. Cazin, C. Vallée, H. Olivier-Bourbigou, P. Braunstein, *Dalton Trans.* 19 (2009) 3824–3832.
- [15] M.T. Zamora, M.J. Ferguson, R. McDonald, M. Cowie, *Dalton Trans.* (2009) 7269–7287.
- [16] M. Raynal, C.S.J. Cazin, C. Vallée, H. Olivier-Bourbigou, P. Braunstein, *Organometallics* 28 (2009) 2460–2470.
- [17] B. Liu, W. Chen, S. Jin, *Organometallics* 26 (2007) 3660–3667.
- [18] D.H. Brown, G.L. Nealon, P.V. Simpson, B.W. Skelton, Z. Wang, *Organometallics* 28 (2009) 1965–1968.
- [19] A.T. Norm, K.J. Cavell, *Eur. J. Inorg. Chem.* 6 (2008) 2781–2880.
- [20] D.J. Nielsen, K.J. Cavell, B.W. Skelton, A.H. White, *Organometallics* 25 (2006) 4850–4856.
- [21] A.A.D. Tulloch, A.A. Danopoulos, G.J. Tizzard, S.J. Coles, M.B. Hursthouse, R.S.H. Motherwell, W.B. Motherwell, *Chem. Commun.* (2001) 1270–1271.
- [22] X.Q. Zhang, Y.P. Qiu, B. Rao, M.M. Luo, *Organometallics* 28 (2009) 3093–3099.
- [23] Q.X. Liu, H. Wang, X.J. Zhao, Z.Q. Yao, Z.Q. Wang, A.H. Chen, X.G. Wang, *CrystEngComm* 14 (2012) 5330–5348.
- [24] C. Marshall, M.F. Ward, W.T.A. Harrison, *J. Organomet. Chem.* 690 (2005) 3970–3975.
- [25] H. Clavier, J.C. Guillemin, M. Mauduit, *Chirality* 19 (2007) 471–476.
- [26] M.S. Jeletic, I. Ghiviriga, K.A. Abboud, A.S. Veige, *Organometallics* 26 (2007) 5267–5270.
- [27] L.G. Bonnet, R.E. Douthwaite, R. Hodgson, *Organometallics* 22 (2003) 4384–4386.
- [28] J.W. Wang, Q.S. Li, F.B. Xu, H.B. Song, Z.Z. Zhang, *Eur. J. Org. Chem.* 5 (2006) 1310–1316.
- [29] Q.X. Liu, X.Q. Yang, X.J. Zhao, S.S. Ge, S.W. Liu, Y. Zang, H.B. Song, J.H. Guo, X.G. Wang, *CrystEngComm* 12 (2010) 2245–2255.
- [30] J.C. Garrison, W.J. Youn, *Chem. Rev.* 105 (2005) 3978–4008.
- [31] F.E. Hahn, M.C. Jahnke, T. Pape, *Organometallics* 25 (2006) 5927–5936.
- [32] M.C. Jahnke, J. Paley, F. Hupka, J.J. Weigand, F.E.Z. Hahn, *Naturforsch* 64b (2009) 1458–1462.
- [33] U.J. Scheele, S. Dechert, F. Meyer, *Inorg. Chim. Acta* 359 (2006) 4891–4900.
- [34] K.M. Lee, J.C.C. Chen, C.J. Huang, I.J.B. Lin, *CrystEngComm* 9 (2007) 278–281.
- [35] Q.X. Liu, L.N. Yin, J.C. Feng, *J. Organomet. Chem.* 692 (2007) 3655–3663.
- [36] L. Ray, M.M. Shaikh, P. Ghosh, *Organometallics* 26 (2007) 958–964.
- [37] A.R. Chianese, P.T. Bremer, C. Wong, R.J. Reynes, *Organometallics* 28 (2009) 5244–5252.
- [38] W.N.O. Wylie, A.J. Lough, R.H. Morris, *Organometallics* 29 (2010) 570–581.
- [39] X. Wang, S. Liu, L.H. Weng, G.X. Jin, *Organometallics* 25 (2006) 3565–3569.
- [40] W.A. Herrmann, S.K. Schneider, K. Öfele, M. Sakamoto, E. Herdtweck, *J. Organomet. Chem.* 689 (2004) 2441–2449.
- [41] J.J. Van Veldhuizen, J.E. Campbell, R.E. Giudici, A.H. Hoveyda, *J. Am. Chem. Soc.* 127 (2005) 6877–6882.
- [42] K.S. Coleman, H.T. Chamberlayne, S. Turberville, M.L.H. Green, A.R. Cowley, *Dalton Trans.* 14 (2003) 2917–2922.
- [43] J.W. Wang, H.B. Song, Q.S. Li, F.B. Xu, Z.Z. Zhang, *Inorg. Chim. Acta* 358 (2005) 3653–3658.
- [44] Y.S. Liu, X.J. Wan, F.B. Xu, *Organometallics* 28 (2009) 5590–5592.
- [45] Q.X. Liu, S.J. Li, X.J. Zhao, Y. Zang, H.B. Song, J.H. Guo, X.G. Wang, *Eur. J. Inorg. Chem.* 6 (2010) 983–988.
- [46] N. Stylianides, A.A. Danopoulos, D. Pugh, F. Hancock, A. Zanotti-Gerosa, *Organometallics* 26 (2007) 5627–5635.
- [47] S. Ahrens, A. Zeller, M. Taige, T. Strassner, *Organometallics* 25 (2006) 5409–5415.
- [48] S.P. Nolan, *N-Heterocyclic Carbenes in Synthesis*, Wiley-VCH Verlag GmbH & Co. KGaA, Weinheim, 2006.
- [49] E.A.B. Kantchev, C.J. O'Brien, M.G. Organ, *Angew. Chem. Int. Ed.* 46 (2007) 2768–2813.
- [50] W.A. Herrmann, *Angew. Chem. Int. Ed.* 41 (2002) 1290–1309.
- [51] W. Wei, M.Y. Wu, Y.G. Huang, Q. Gao, F.L. Jiang, M.C. Hong, Z. Anorg. Allg. Chem. 634 (2008) 2623–2628.
- [52] H. William, G.O. Allen, *Acta Cryst. C* 55 (1999) 1406–1408.
- [53] A.D. Pra, G. Zanotti, G. Bombieri, R. Ros, *Inorg. Chim. Acta* 36 (1979) 121–125.
- [54] R. McCrindle, G. Ferguson, A.J. McAlees, M. Parvez, P.J. Roberts, *J. Chem. Soc. Dalton Trans.* 9 (1982) 1699–1708.
- [55] P.S. Pregosin, *Inorg. Chim. Acta* 45 (1980) 7–9.
- [56] S. Inoue, Y. Sato, *Organometallics* 5 (1986) 1197–1201.
- [57] Q.X. Liu, A.H. Chen, X.J. Zhao, Y. Zang, X.M. Wu, X.G. Wang, *J.H. Guo, CrystEngComm* 13 (2011) 293–305.
- [58] F. Weller, *Z. Anorg. Allg. Chem.* 415 (1975) 233–240.
- [59] B. Luigi, B. Silvia, Z. Valerio, A.G. Vincenzo, B. Dario, *New J. Chem.* 16 (1992) 693–696.
- [60] K.M. Lee, J.C.C. Chen, I.J.B. Lin, *J. Organomet. Chem.* 364 (2001) 617–618.
- [61] T. Weskamp, V.P.W. Böhm, W.A. Herrmann, *J. Organomet. Chem.* 600 (2000) 12–22.
- [62] J.C. Garrison, R.S. Simons, J.M. Talley, C. Wesdemiotis, C.A. Tessier, W.J. Youn, *Organometallics* 20 (2001) 1276–1278.
- [63] A. Caballero, E. Díez-Barra, F.A. Jalón, S. Merino, J. Tejada, *J. Organomet. Chem.* 395 (2001) 617–618.
- [64] L. Pauling, *The Nature of the Chemical Bond*, third ed., Cornell University Press, Ithaca, N.Y., 1960, pp. 269.
- [65] C. Juan, R. Mareque, B. Lee, *Coord. Chem. Rev.* 183 (1999) 43–80.
- [66] N.L. Rosi, J. Kim, M. Eddaoudi, B. Chen, M. O'Keefe, O.M. Yaghi, *J. Am. Chem. Soc.* 127 (2005) 1504–1508.
- [67] A.R. Choudhury, R.G. Bhat, T.N.G. Row, S. Chandrasekaran, *Cryst. Growth Des.* 7 (2007) 844–866.
- [68] L. Brammer, E.A. Bruton, P. Sherwood, *Cryst. Growth Des.* 1 (2001) 277–290.
- [69] V.R. Thalladi, H.C. Weiss, D. Balser, R. Boese, A. Nangia, G.R. Desiraju, *J. Am. Chem. Soc.* 120 (1998) 8702–8710.
- [70] T. Steiner, W. Saenger, *J. Am. Chem. Soc.* 114 (1992) 10146–10154.
- [71] R.T. Edward Tiekink, J. Zukerman-Schpector, *The Importance of Pi-Interactions in Crystal Engineering: Frontiers in Crystal Engineering*, 1st ed., John Wiley & Sons, Ltd, 2012.
- [72] Y.S. Chong, W.R. Carroll, W.G. Burns, M.D. Smith, K.D. Shimizu, *Chem. Eur. J.* 15 (2009) 9117–9126.
- [73] F. Neve, A. Crispini, *CrystEngComm* 5 (2003) 265–268.
- [74] L. Rajput, K. Biradha, *CrystEngComm* 11 (2009) 1220–1222.
- [75] S.F. Alshahateet, R. Bishop, D.C. Craig, M.L. Scudder, *CrystEngComm* 48 (2001) 1–5.
- [76] S.E. Snyder, B.S. Huang, Y.W. Chu, H.S. Lin, J.R. Carey, *Chem. Eur. J.* 18 (2012) 12663–12671.
- [77] C.A. Hunter, K.R. Lawson, J. Perkins, C.J. Urch, *J. Chem. Soc. Perkin Trans. 2* (2001) 651–669.
- [78] C.S. Lai, F. Mohr, E.R. Edward Tiekink, *CrystEngComm* 8 (2006) 909–915.
- [79] R.P.A. Bettens, D. Dakternieks, A. Duthie, F.S. Kuan, E.R. Edward Tiekink, *CrystEngComm* 11 (2009) 1362–1372.
- [80] G.R. Desiraju, T. Steiner, *The Weak Hydrogen Bond in Structural Chemistry and Biology*, Oxford University Press, Oxford, UK, 1999.
- [81] A.L. Pickering, G. Seeber, D.L. Long, L. Cronin, *CrystEngComm* 7 (2005) 504–510.
- [82] F. Artuso, A.A. D'Archivio, S. Lora, K. Jerabek, M. Králík, B. Corain, *Chem. Eur. J.* 9 (2003) 5292–5296.
- [83] T. Teranishi, M. Miyake, *Chem. Mater.* 10 (1998) 594–600.
- [84] A. Zanardi, J.A. Mata, E. Peris, *Organometallics* 28 (2009) 4335–4339.
- [85] S.K. Yen, L.L. Koh, H.V. Huynh, T.S.A. Hor, *Chem. Asian J.* 3 (2008) 1649–1656.
- [86] N.D. Jones, B.R. James, *Adv. Synth. Catal.* 344 (2002) 1126–1134.
- [87] C.M. Jin, B. Twamley, J.M. Shreeve, *Organometallics* 24 (2005) 3020–3023.

- [88] D. Kremzow, G. Seidel, C.W. Lehmann, A. Fürstner, *Chem. Eur. J.* 11 (2005) 1833–1853.
- [89] Y. Gök, N. Gürbüz, I. Özdemir, B. Çetinkaya, E. Çetinkaya, *Appl. Organometal. Chem.* 19 (2005) 870–874.
- [90] F.J.B. dit Dominique, H. Gornitzka, S.A. Sournia, C. Hemmert, *Dalton Trans.* (2009) 340–352.
- [91] V.J. Catalano, A.L. Moore, *Inorg. Chem.* 44 (2005) 6558–6566.
- [92] F.J.B. dit Dominique, H. Gornitzka, A. Sournia-Saquet, C. Hemmert, *Dalton Trans.* 2 (2009) 340–352.
- [93] A.P. de Silva, H.Q.N. Lgunaratne, T.L. Gunnlangsson, A.J.M. Unzley, C.P. McCoy, J.T. Rademacher, T.E. Rice, *Chem. Rev.* 97 (1997) 1515–1566.
- [94] SMART 5.0 and SAINT 4.0 for Windows NT, Area Detector Control and Integration Software, Bruker Analytical X-Ray Systems, Inc., Madison, WI, USA, 1998.
- [95] G.M. Sheldrick, SADABS, Program for Empirical Absorption Correction of Area Detector Data, Univ. of Göttingen, Germany, 1996.
- [96] G.M. Sheldrick, SHELXTL 5.10 for Windows NT, Structure Determination Software, Bruker Analytical X-Ray Systems, Inc., Madison, WI, USA, 1997.